Supporting information

Determine Packing Model of a Supramolecular Nanofiber *via* Mass-per-Length Measurement and *de novo* Simulation

Qingxin Yao, Qiang Bao, Xinming Li, Hui Wang, Zhenyu Yang, Xinghua Shi, Yuan Gao and Bing Xu

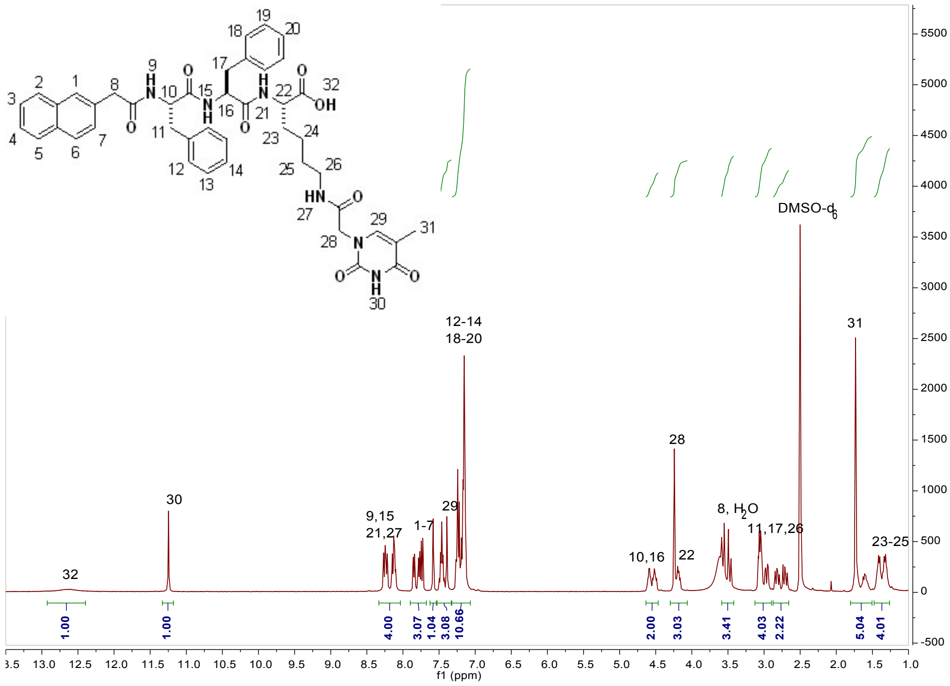

Figure S1. The ^{1}H NMR of NapFFK_Thy (**1**).

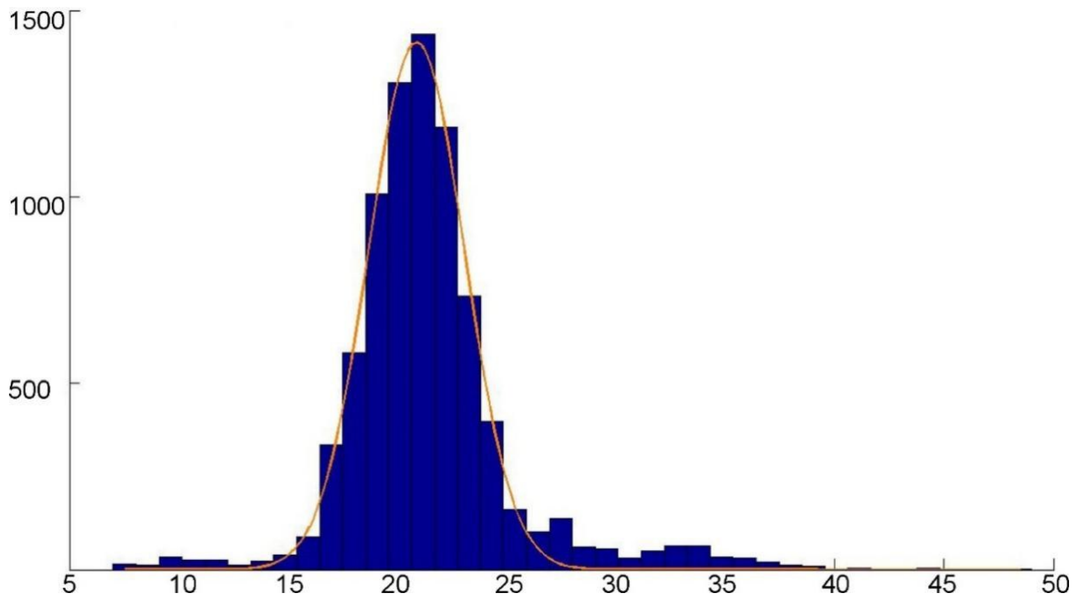

Figure S2. The widths spreads of the filtered and initially aligned NapFFK_Thy (**1**) nanofiber samples. The y-axis is number of images and x-axis is the width in units of pixels. The Phillips CM12 electron microscope is 120 kV electron microscope that uses a LaB6 electron source and a Gatan UltraScan 1000 2K by 2k pixel CCD bottom mounted camera. The nominal magnification of these images was 35000X with a defocus of 1.5 μm and a pixel size of 3.04Å.

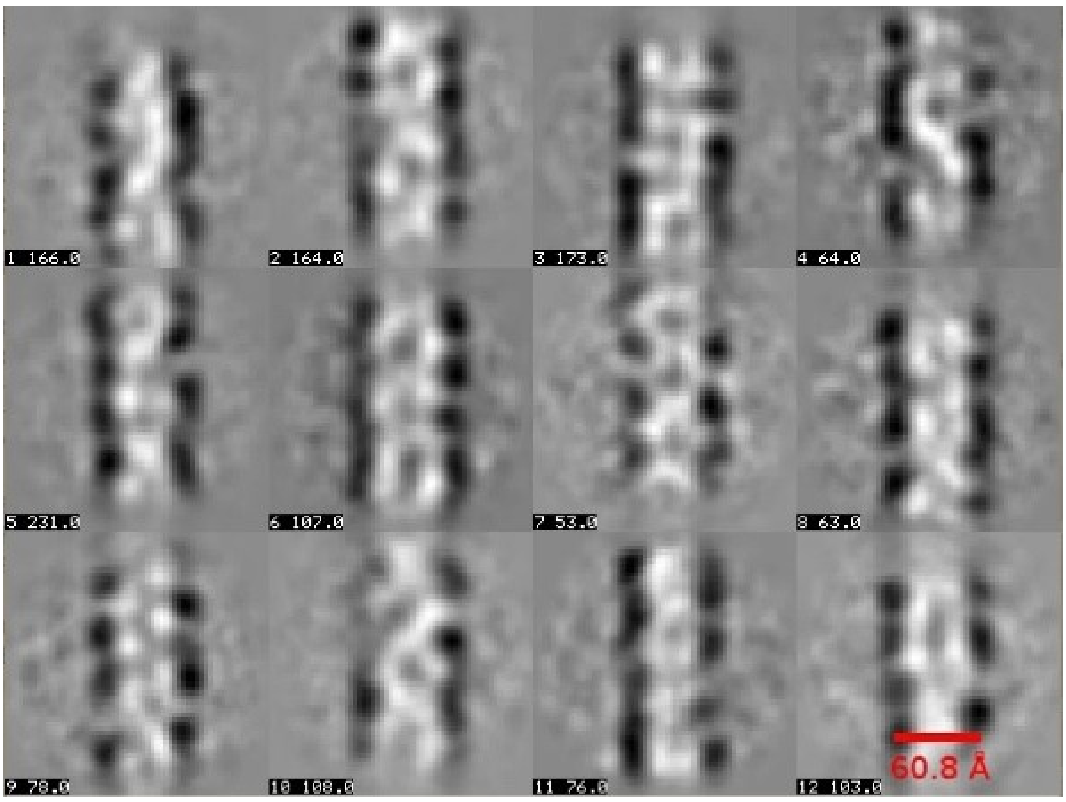

Figure S3. Sample of the structures found in the NapFFK_Thy (**1**) nanofibers. Single particle reconstruction to reveal the polymorphorism nature of supramolecular nanofibers.

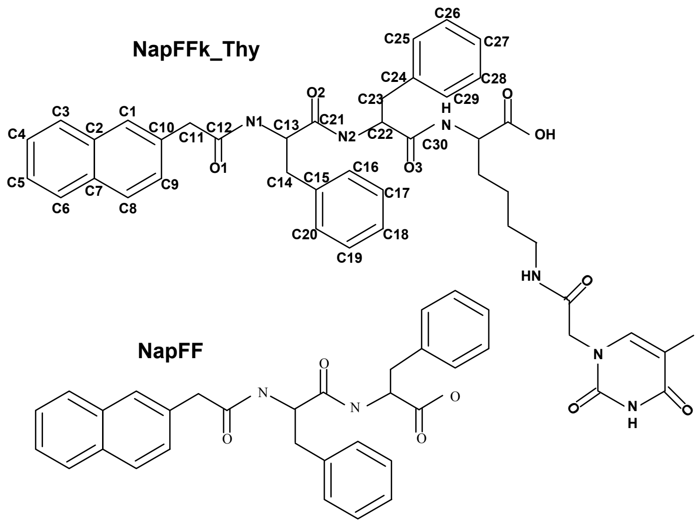

Figure S4. The molecular structures of NapFFK_Thy (**1**) and NapFF.

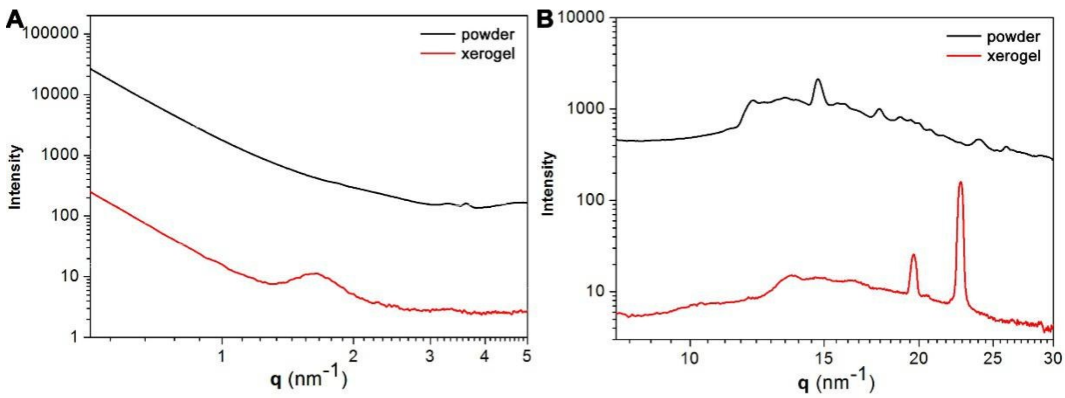

Figure S5. (A) SAXS and (B) WAXS measurements of the lyophilized powder and xerogel of **1**. The peak at q=1.6 nm^{-1} indicated the formation of nanofibers at a regular diameter though it was a little smaller than that determined by TEM. This discrepancy may be due to the shrinkage in the xerogel. The peaks at q=19.7 nm^{-1} and 22.7 nm^{-1} indicated two distinct patterns in π-π interaction.

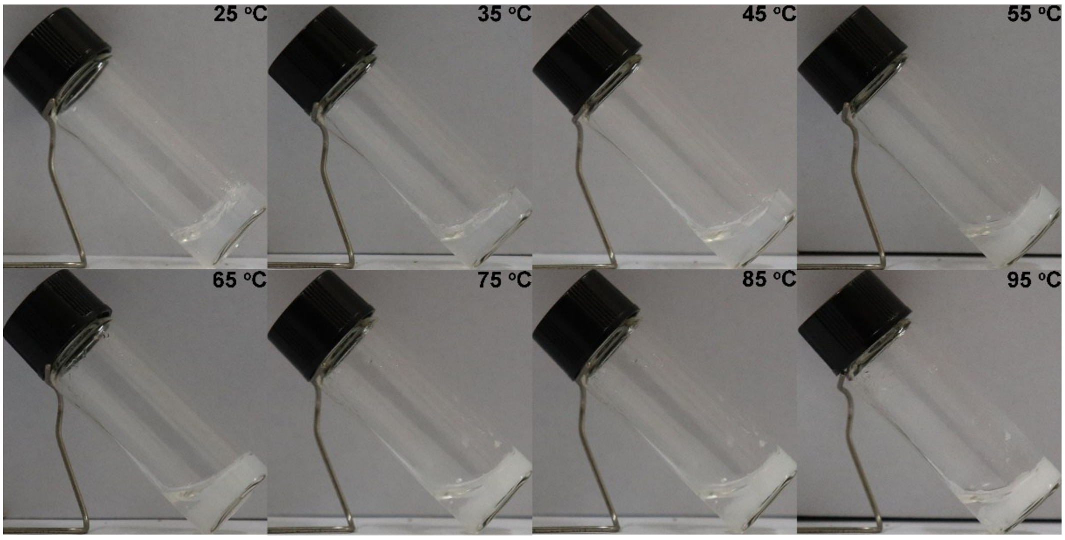

Figure S6. The optical images showed the collapse of the hydrogel of **1** during heating in water bath.

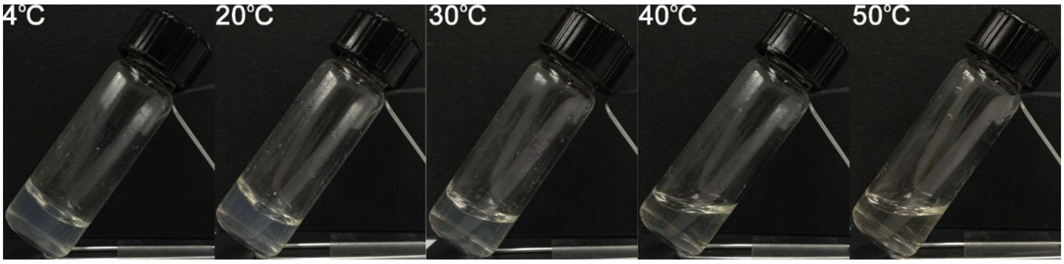

Figure S7. The optical images showed the dissolving of the hydrogel of NapFFKYp [1] during heating in water bath.

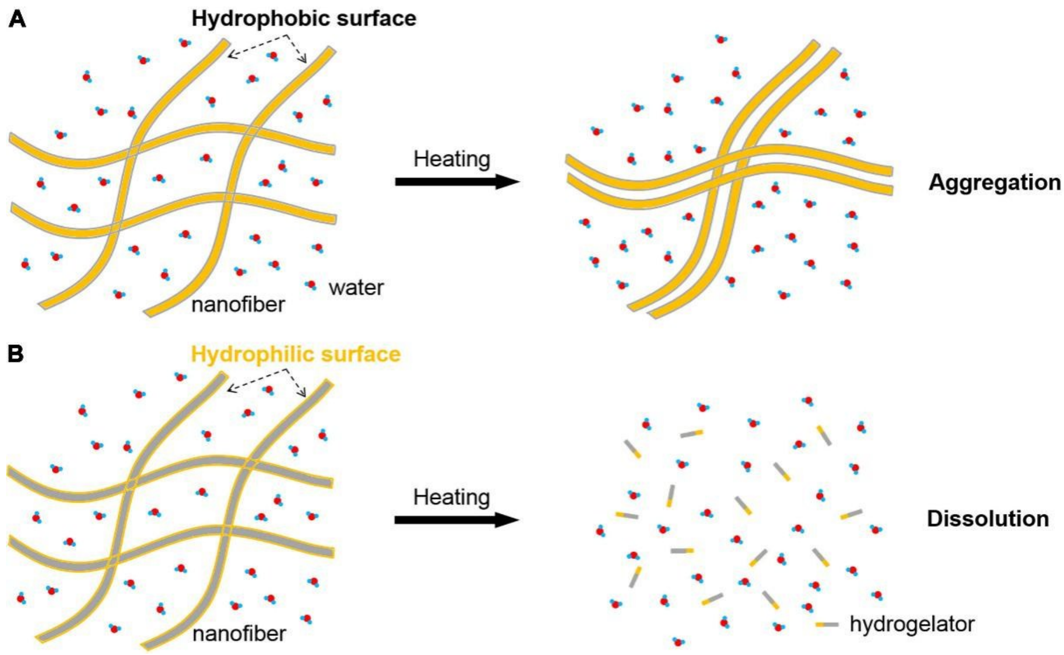

Figure S8. The interpretative scheme showed the phenomena of (A) aggregation for **1** and (B) dissolution for NapFFKYp during heating the nanofibers with different surface.

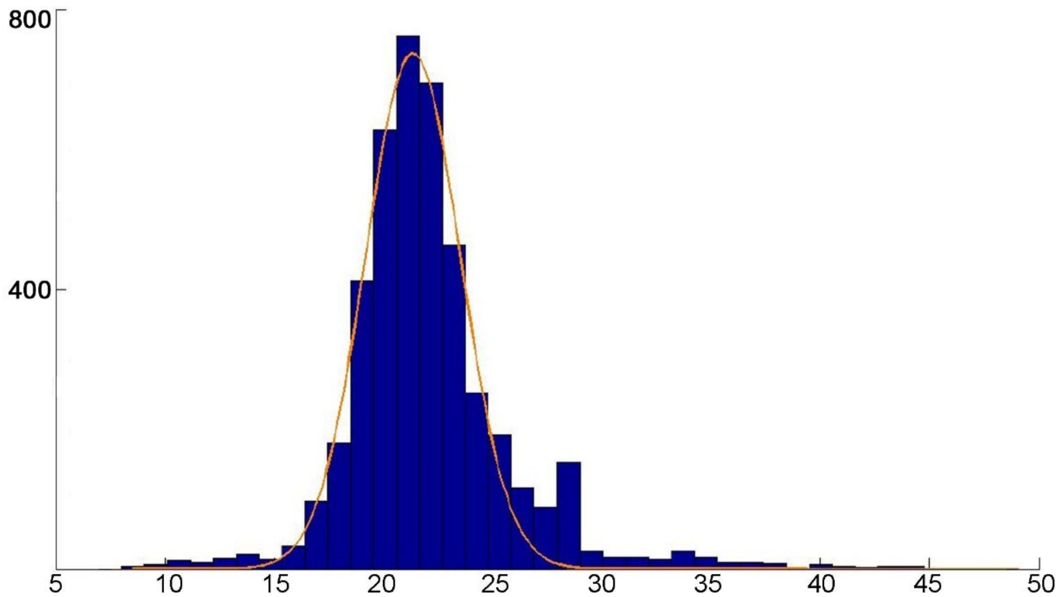

Figure S9. The widths spreads of the filtered and initially aligned NapFFK_Thy (1) with poly-A_{16} nanofiber samples. Each pixel equals to 3.04Å.

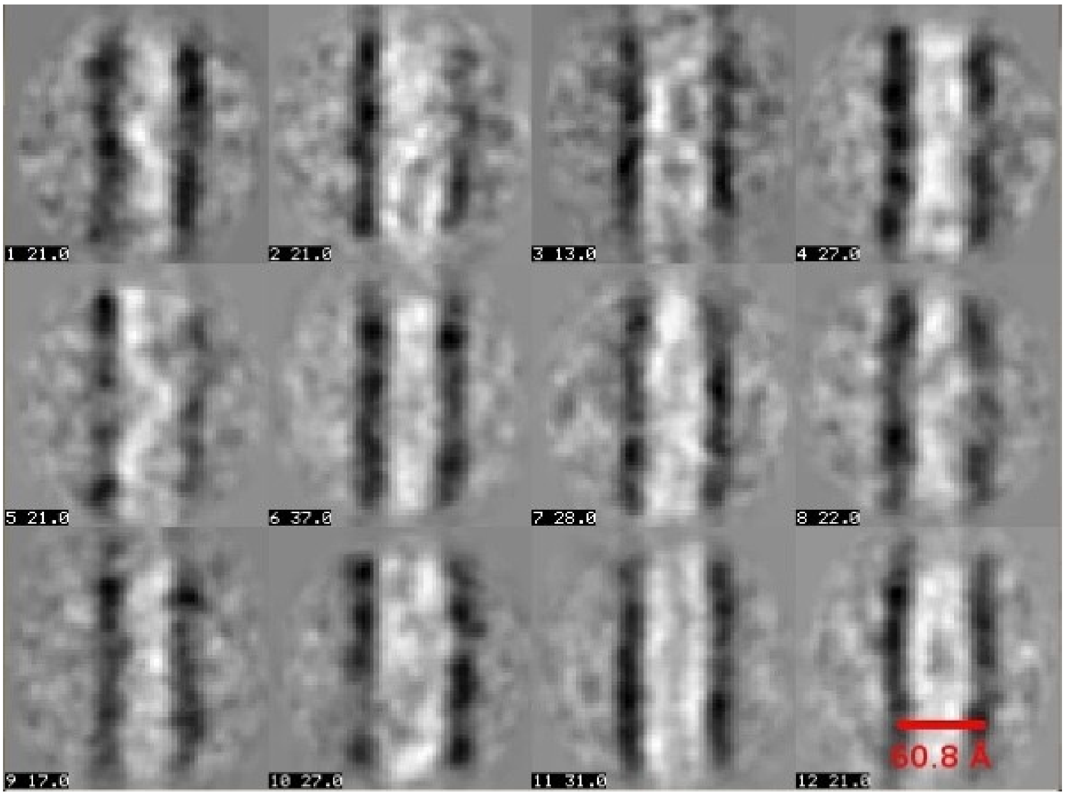

Figure S10. Sample of the structures found in the NapFFK_Thy (1) with poly-A_{16} nanofibers.

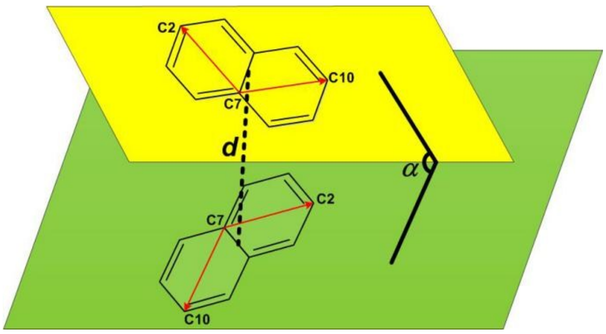

Figure S11. The scheme showed centroid distance *d* and angle *α* between two naphthalene ring planes.

Three non-colliner atoms belong to the naphthalene ring named C10, C7, C2 were used to calculate the normal vector ***n*** of the ring plane, as shown in Figure S9. The normal vector of each plane could be calculated by

$$\vec{n} = \overrightarrow{C7C10} \times \overrightarrow{C7C2} \tag{1}$$

Then angle of two plane α was obtained by

$$\alpha = 90° - \arccos\frac{\vec{n}_1 \cdot \vec{n}_2}{|\vec{n}_1||\vec{n}_2|} \qquad (0° \leq \alpha \leq 90°) \tag{2}$$

$\boldsymbol{n}_i$ (i=1, 2) were the normal vector of two planes. Here, only the centroid distance of two naphthalene rings below 0.7 nm were counted.

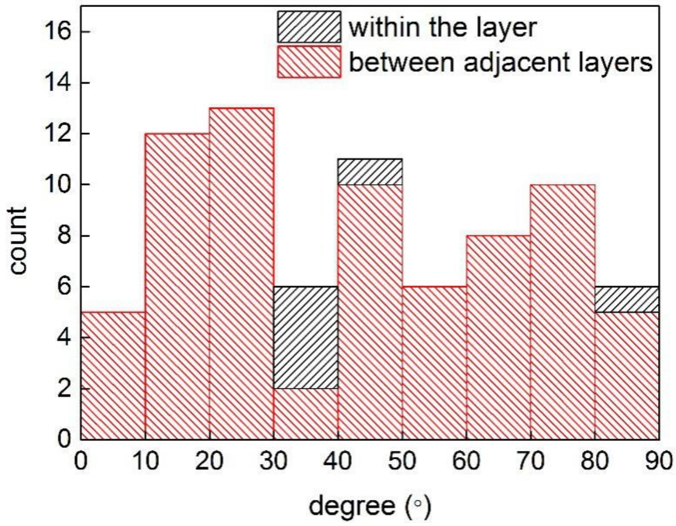

Figure S12. The distribution of all the possible π-π interaction with the angle between two naphthalene ring planes.

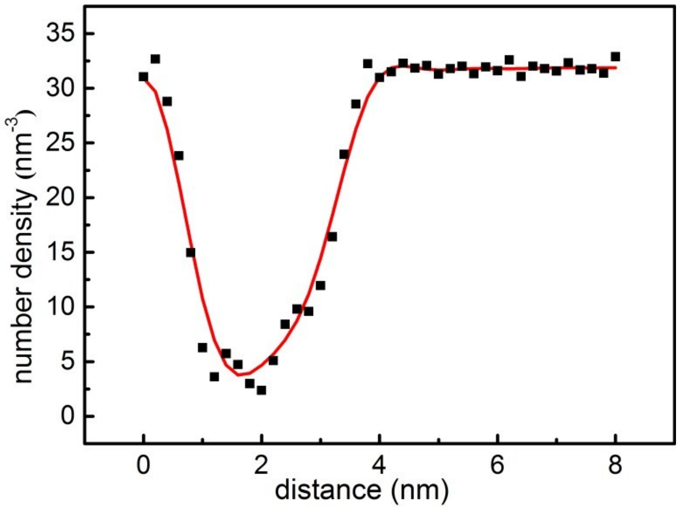

Figure S13. The number density distribution of water molecules along the radial direction of the nanofiber. The red line represents the smoothed results.

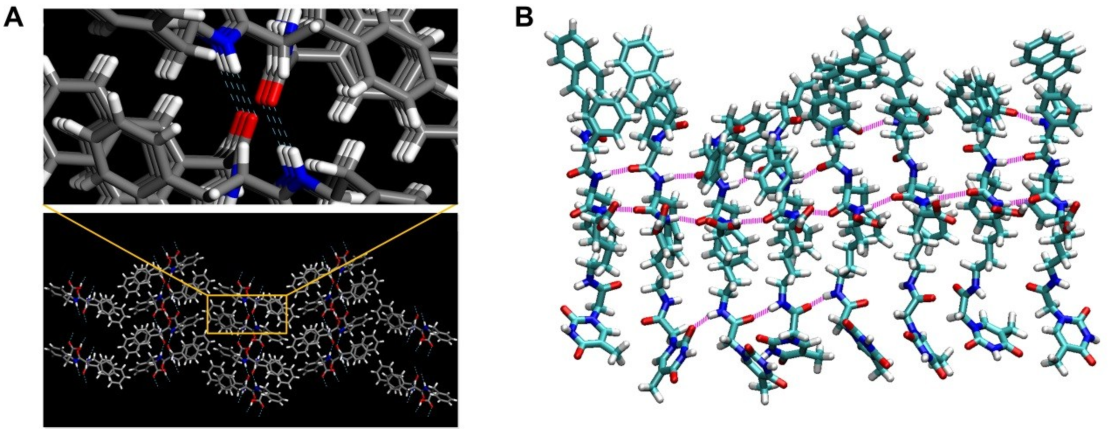

Figure S14. The hydrogen bonds in (A) NapFF crystal structure (blue dashed line) and (B) the nanofiber along the fiber axial direction (magenta color) showed similar hydrogen bonding interaction and β-sheets.

Table S1. The force field parameters for the molecule NapFFK_Thy

[**moleculetype**]

Name	nrexcl
Protein	3

[atom]

nr	type	resnr	resid	atom	cgnr	charge	mass
1	HS14	1	863V	H30	1	0.479158	1.008
2	OA	1	863V	O4	1	-0.7001	15.9994
3	C	1	863V	C32	2	0.776342	12.011
4	O	1	863V	O5	2	-0.5973	15.9994
5	C	1	863V	C31	2	0.173723	12.011
6	HC	1	863V	H29	2	0.102512	1.008
7	N	1	863V	N3	2	-0.5981	14.0067
8	HS14	1	863V	H28	2	0.272954	1.008
9	C	1	863V	C30	3	0.615254	12.011
10	O	1	863V	O3	3	-0.59627	15.9994
11	C	1	863V	C22	4	0.223151	12.011
12	HC	1	863V	H20	4	0.0607	1.008
13	N	1	863V	N2	4	-0.61538	14.0067
14	HS14	1	863V	H19	4	0.324467	1.008
15	C	1	863V	C21	4	0.596426	12.011
16	O	1	863V	O2	4	-0.57217	15.9994
17	C	1	863V	C13	5	0.309322	12.011
18	HC	1	863V	H11	5	0.037857	1.008
19	N	1	863V	N1	5	-0.64564	14.0067
20	HS14	1	863V	H10	5	0.318176	1.008
21	C	1	863V	C12	5	0.792346	12.011
22	O	1	863V	O1	5	-0.65249	15.9994
23	C	1	863V	C11	6	-0.48471	12.011
24	HC	1	863V	H8	6	0.158811	1.008
25	HC	1	863V	H9	6	0.158811	1.008
26	C	1	863V	C10	6	0.315867	12.011
27	C	1	863V	C9	6	-0.30753	12.011
28	HC	1	863V	H7	6	0.185279	1.008
29	C	1	863V	C8	7	-0.2232	12.011
30	HC	1	863V	H6	7	0.170674	1.008
31	C	1	863V	C7	7	0.159999	12.011
32	C	1	863V	C6	7	-0.26194	12.011
33	HC	1	863V	H5	7	0.161199	1.008
34	C	1	863V	C5	8	-0.11214	12.011
35	HC	1	863V	H4	8	0.141423	1.008
36	C	1	863V	C4	8	-0.1449	12.011

37	HC	1	863V	H3	8	0.147277	1.008
38	C	1	863V	C3	9	-0.24061	12.011
39	HC	1	863V	H2	9	0.154561	1.008
40	C	1	863V	C2	9	0.200642	12.011
41	C	1	863V	C1	9	-0.41406	12.011
42	HC	1	863V	H1	9	0.18205	1.008
43	C	1	863V	C14	10	-0.34847	12.011
44	HC	1	863V	H12	10	0.113127	1.008
45	HC	1	863V	H13	10	0.113127	1.008
46	C	1	863V	C15	10	0.227078	12.011
47	C	1	863V	C16	10	-0.24154	12.011
48	HC	1	863V	H14	10	0.154578	1.008
49	C	1	863V	C20	11	-0.24154	12.011
50	HC	1	863V	H18	11	0.154578	1.008
51	C	1	863V	C19	11	-0.11882	12.011
52	HC	1	863V	H17	11	0.138517	1.008
53	C	1	863V	C18	12	-0.16352	12.011
54	HC	1	863V	H16	12	0.140692	1.008
55	C	1	863V	C17	12	-0.11882	12.011
56	HC	1	863V	H15	12	0.138517	1.008
57	C	1	863V	C23	13	-0.20281	12.011
58	HC	1	863V	H21	13	0.087664	1.008
59	HC	1	863V	H22	13	0.087664	1.008
60	C	1	863V	C24	13	0.080538	12.011
61	C	1	863V	C29	13	-0.1778	12.011
62	HC	1	863V	H27	13	0.127785	1.008
63	C	1	863V	C25	14	-0.1778	12.011
64	HC	1	863V	H23	14	0.127785	1.008
65	C	1	863V	C26	14	-0.09543	12.011
66	HC	1	863V	H24	14	0.126106	1.008
67	C	1	863V	C27	15	-0.18576	12.011
68	HC	1	863V	H25	15	0.140718	1.008
69	C	1	863V	C28	15	-0.09543	12.011
70	HC	1	863V	H26	15	0.126106	1.008
71	C	1	863V	C33	16	-0.16424	12.011
72	HC	1	863V	H31	16	0.085632	1.008
73	HC	1	863V	H32	16	0.085632	1.008
74	C	1	863V	C34	17	-0.05777	12.011
75	HC	1	863V	H33	17	0.032692	1.008
76	HC	1	863V	H34	17	0.032692	1.008
77	C	1	863V	C35	17	-0.09878	12.011
78	HC	1	863V	H35	17	0.046957	1.008
79	HC	1	863V	H36	17	0.046957	1.008
80	C	1	863V	C36	18	0.214389	12.011

81	HC	1	863V	H37	18	0.052935	1.008
82	HC	1	863V	H38	18	0.052935	1.008
83	N	1	863V	N4	18	-0.82805	14.0067
84	HS14	1	863V	H39	18	0.425705	1.008
85	C	1	863V	C37	18	0.822205	12.011
86	O	1	863V	O6	18	-0.61527	15.9994
87	C	1	863V	C38	19	-0.24581	12.011
88	HC	1	863V	H40	19	0.11791	1.008
89	HC	1	863V	H41	19	0.11791	1.008
90	NT	1	863V	N5	19	-0.08813	14.0067
91	C	1	863V	C43	20	0.772388	12.011
92	O	1	863V	O8	20	-0.63119	15.9994
93	N	1	863V	N6	21	-0.73969	14.0067
94	HS14	1	863V	H46	21	0.410352	1.008
95	C	1	863V	C42	21	0.773478	12.011
96	O	1	863V	O7	21	-0.58086	15.9994
97	C	1	863V	C40	22	-0.08238	12.011
98	C	1	863V	C39	22	-0.14907	12.011
99	HC	1	863V	H42	22	0.218631	1.008
100	C	1	863V	C41	22	-0.36353	12.011
101	HC	1	863V	H43	22	0.122018	1.008
102	HC	1	863V	H44	22	0.122018	1.008
103	HC	1	863V	H45	22	0.122018	1.008

[bonds]

ai	aj	funct	c0	c1
1	2	2	0.0972	1.96E+07
2	3	2	0.136	1.02E+07
3	4	2	0.123	1.66E+07
3	5	2	0.152	5.43E+06
5	6	2	0.114	3.85E+07
5	7	2	0.1435	6.10E+06
5	71	2	0.154	4.22E+06
7	8	2	0.1	1.87E+07
7	9	2	0.138	1.10E+07
9	10	2	0.125	1.34E+07
9	11	2	0.154	4.22E+06
11	12	2	0.114	3.85E+07
11	13	2	0.1435	6.10E+06
11	57	2	0.154	4.22E+06
13	14	2	0.1	1.87E+07
13	15	2	0.138	1.10E+07
15	16	2	0.125	1.34E+07
15	17	2	0.156	3.08E+06
17	18	2	0.113	7.05E+06
17	19	2	0.1435	6.10E+06
17	43	2	0.153	7.15E+06
19	20	2	0.1	1.87E+07
19	21	2	0.138	1.10E+07
21	22	2	0.125	1.34E+07
21	23	2	0.152	5.43E+06
23	24	2	0.113	7.05E+06
23	25	2	0.112	3.70E+07
23	26	2	0.149	1.42E+07
26	27	2	0.142	3.22E+06
26	41	2	0.138	1.10E+07
27	28	2	0.11	1.21E+07
27	29	2	0.138	1.10E+07
29	30	2	0.11	1.21E+07
29	31	2	0.142	3.22E+06
31	32	2	0.142	3.22E+06
31	40	2	0.142	3.22E+06
32	33	2	0.11	1.21E+07
32	34	2	0.138	1.10E+07
34	35	2	0.11	1.21E+07
34	36	2	0.142	3.22E+06
36	37	2	0.11	1.21E+07
36	38	2	0.138	1.10E+07

38	39	2	0.11	1.21E+07
38	40	2	0.142	3.22E+06
40	41	2	0.142	3.22E+06
41	42	2	0.11	1.21E+07
43	44	2	0.112	3.70E+07
43	45	2	0.112	3.70E+07
43	46	2	0.149	1.42E+07
46	47	2	0.139	8.66E+06
46	49	2	0.14	8.54E+06
47	48	2	0.11	1.21E+07
47	55	2	0.139	8.66E+06
49	50	2	0.11	1.21E+07
49	51	2	0.139	8.66E+06
51	52	2	0.109	1.23E+07
51	53	2	0.139	8.66E+06
53	54	2	0.109	1.23E+07
53	55	2	0.139	8.66E+06
55	56	2	0.109	1.23E+07
57	58	2	0.112	3.70E+07
57	59	2	0.112	3.70E+07
57	60	2	0.149	1.42E+07
60	61	2	0.14	8.54E+06
60	63	2	0.139	8.66E+06
61	62	2	0.11	1.21E+07
61	69	2	0.139	8.66E+06
63	64	2	0.11	1.21E+07
63	65	2	0.139	8.66E+06
65	66	2	0.11	1.21E+07
65	67	2	0.139	8.66E+06
67	68	2	0.109	1.23E+07
67	69	2	0.139	8.66E+06
69	70	2	0.109	1.23E+07
71	72	2	0.112	3.70E+07
71	73	2	0.112	3.70E+07
71	74	2	0.152	5.43E+06
74	75	2	0.112	3.70E+07
74	76	2	0.112	3.70E+07
74	77	2	0.152	5.43E+06
77	78	2	0.112	3.70E+07
77	79	2	0.112	3.70E+07
77	80	2	0.153	7.15E+06
80	81	2	0.113	7.05E+06
80	82	2	0.113	7.05E+06
80	83	2	0.1435	6.10E+06

83	84	2	0.1	1.87E+07
83	85	2	0.138	1.10E+07
85	86	2	0.125	1.34E+07
85	87	2	0.154	4.22E+06
87	88	2	0.113	7.05E+06
87	89	2	0.113	7.05E+06
87	90	2	0.1435	6.10E+06
90	91	2	0.142	3.22E+06
90	98	2	0.139	8.66E+06
91	92	2	0.125	1.34E+07
91	93	2	0.14	8.54E+06
93	94	2	0.1	1.87E+07
93	95	2	0.14	8.54E+06
95	96	2	0.125	1.34E+07
95	97	2	0.148	5.73E+06
97	98	2	0.136	1.02E+07
97	100	2	0.148	5.73E+06
98	99	2	0.111	4.87E+06
100	101	2	0.112	3.70E+07
100	102	2	0.112	3.70E+07
100	103	2	0.112	3.70E+07

[pairs]; all 1-4 pairs but the ones excluded in GROMOS itp

ai	aj	funct
1	4	1
1	5	1
2	6	1
2	7	1
2	71	1
3	8	1
3	9	1
3	72	1
3	73	1
3	74	1
4	6	1
4	7	1
4	71	1
5	10	1
5	11	1
5	75	1
5	76	1
5	77	1
6	8	1
6	9	1
6	72	1
6	73	1
6	74	1
7	12	1
7	13	1
7	57	1
7	72	1
7	73	1
7	74	1
8	10	1
8	11	1
8	71	1
9	14	1
9	15	1
9	58	1
9	59	1
9	60	1
9	71	1
10	12	1
10	13	1
10	57	1
11	16	1

11	17	1
11	61	1
11	63	1
12	14	1
12	15	1
12	58	1
12	59	1
12	60	1
13	18	1
13	19	1
13	43	1
13	58	1
13	59	1
13	60	1
14	16	1
14	17	1
14	57	1
15	20	1
15	21	1
15	44	1
15	45	1
15	46	1
15	57	1
16	18	1
16	19	1
16	43	1
17	22	1
17	23	1
17	47	1
17	49	1
18	20	1
18	21	1
18	44	1
18	45	1
18	46	1
19	24	1
19	25	1
19	26	1
19	44	1
19	45	1
19	46	1
20	22	1
20	23	1
20	43	1

21	27	1
21	41	1
21	43	1
22	24	1
22	25	1
22	26	1
23	28	1
23	29	1
23	40	1
23	42	1
24	27	1
24	41	1
25	27	1
25	41	1
26	30	1
27	42	1
28	30	1
28	31	1
28	41	1
29	33	1
30	32	1
30	40	1
31	35	1
31	39	1
31	42	1
32	37	1
33	35	1
33	36	1
33	40	1
34	39	1
35	37	1
35	38	1
37	39	1
37	40	1
38	42	1
39	41	1
43	48	1
43	50	1
43	51	1
43	55	1
44	47	1
44	49	1
45	47	1
45	49	1

46	52	1
46	56	1
47	50	1
47	54	1
48	49	1
48	53	1
48	56	1
49	54	1
50	52	1
50	53	1
51	56	1
52	54	1
52	55	1
54	56	1
57	62	1
57	64	1
57	65	1
57	69	1
58	61	1
58	63	1
59	61	1
59	63	1
60	66	1
60	70	1
61	64	1
61	68	1
62	63	1
62	67	1
62	70	1
63	68	1
64	66	1
64	67	1
65	70	1
66	68	1
66	69	1
68	70	1
71	78	1
71	79	1
71	80	1
72	75	1
72	76	1
72	77	1
73	75	1
73	76	1

73	77	1
74	81	1
74	82	1
74	83	1
75	78	1
75	79	1
75	80	1
76	78	1
76	79	1
76	80	1
77	84	1
77	85	1
78	81	1
78	82	1
78	83	1
79	81	1
79	82	1
79	83	1
80	86	1
80	87	1
81	84	1
81	85	1
82	84	1
82	85	1
83	88	1
83	89	1
83	90	1
84	86	1
84	87	1
85	91	1
85	98	1
86	88	1
86	89	1
86	90	1
87	92	1
87	93	1
87	97	1
87	99	1
88	91	1
88	98	1
89	91	1
89	98	1
90	94	1
90	100	1

91	96	1
91	99	1
92	94	1
92	95	1
92	98	1
93	100	1
94	96	1
94	97	1
95	99	1
95	101	1
95	102	1
95	103	1
96	98	1
96	100	1
98	101	1
98	102	1
98	103	1
99	100	1

[angles]

ai	aj	ak	funct	angle	fc
1	2	3	2	109.5	450
2	3	4	2	117.2	636
2	3	5	2	115	610
4	3	5	2	126	640
3	5	6	2	108.53	443
3	5	7	2	109.5	520
3	5	71	2	109.5	520
6	5	7	2	108.53	443
6	5	71	2	109	1680.51
7	5	71	2	115	610
5	7	8	2	116	465
5	7	9	2	122	700
8	7	9	2	120	390
7	9	10	2	124	730
7	9	11	2	120	560
10	9	11	2	121	685
9	11	12	2	106	1733.55
9	11	13	2	111	530
9	11	57	2	109.5	520
12	11	13	2	108.53	443
12	11	57	2	108.53	443
13	11	57	2	111	530
11	13	14	2	120	390
11	13	15	2	122	700
14	13	15	2	120	390
13	15	16	2	124	730
13	15	17	2	115	610
16	15	17	2	121	685
15	17	18	2	108	465
15	17	19	2	111	530
15	17	43	2	109.5	520
18	17	19	2	108.53	443
18	17	43	2	108.53	443
19	17	43	2	115	610
17	19	20	2	116	465
17	19	21	2	122	700
20	19	21	2	120	390
19	21	22	2	124	730
19	21	23	2	120	560
22	21	23	2	120	560
21	23	24	2	106.75	503
21	23	25	2	106	1733.55

21	23	26	2	120	560
24	23	25	2	107.57	484
24	23	26	2	109.6	450
25	23	26	2	110.3	524
23	26	27	2	120	560
23	26	41	2	120	560
27	26	41	2	120	560
26	27	28	2	120	505
26	27	29	2	120	560
28	27	29	2	120	505
27	29	30	2	120	505
27	29	31	2	120	560
30	29	31	2	120	505
29	31	32	2	120	560
29	31	40	2	120	560
32	31	40	2	120	560
31	32	33	2	120	505
31	32	34	2	120	560
33	32	34	2	120	505
32	34	35	2	120	505
32	34	36	2	120	560
35	34	36	2	120	505
34	36	37	2	120	505
34	36	38	2	120	560
37	36	38	2	120	505
36	38	39	2	120	505
36	38	40	2	120	560
39	38	40	2	120	505
31	40	38	2	120	560
31	40	41	2	120	560
38	40	41	2	120	560
26	41	40	2	120	560
26	41	42	2	120	505
40	41	42	2	120	505
17	43	44	2	109.6	450
17	43	45	2	107	2726.16
17	43	46	2	111	530
44	43	45	2	106.75	503
44	43	46	2	111	530
45	43	46	2	110	4763.46
43	46	47	2	120	560
43	46	49	2	120	560
47	46	49	2	120	560
46	47	48	2	120	505

46	47	55	2	120	560
48	47	55	2	120	505
46	49	50	2	120	505
46	49	51	2	120	560
50	49	51	2	120	505
49	51	52	2	120	505
49	51	53	2	120	560
52	51	53	2	120	505
51	53	54	2	120	505
51	53	55	2	120	560
54	53	55	2	120	505
47	55	53	2	120	560
47	55	56	2	120	505
53	55	56	2	120	505
11	57	58	2	110.3	524
11	57	59	2	108	465
11	57	60	2	111	530
58	57	59	2	107	2726.16
58	57	60	2	110.3	524
59	57	60	2	109	1680.51
57	60	61	2	120	560
57	60	63	2	120	560
61	60	63	2	120	560
60	61	62	2	120	505
60	61	69	2	120	560
62	61	69	2	120	505
60	63	64	2	120	505
60	63	65	2	120	560
64	63	65	2	120	505
63	65	66	2	120	505
63	65	67	2	120	560
66	65	67	2	120	505
65	67	68	2	120	505
65	67	69	2	120	560
68	67	69	2	120	505
61	69	67	2	120	560
61	69	70	2	120	505
67	69	70	2	120	505
5	71	72	2	109.6	450
5	71	73	2	109	1680.51
5	71	74	2	111	530
72	71	73	2	107.57	484
72	71	74	2	110.3	524
73	71	74	2	109.6	450

71	74	75	2	109	1680.51
71	74	76	2	109.6	450
71	74	77	2	111	530
75	74	76	2	107	2726.16
75	74	77	2	109	1680.51
76	74	77	2	110	4763.46
74	77	78	2	109	1680.51
74	77	79	2	110	4763.46
74	77	80	2	111	530
78	77	79	2	107.57	484
78	77	80	2	109.5	285
79	77	80	2	110.3	524
77	80	81	2	108.53	443
77	80	82	2	109.5	285
77	80	83	2	115	610
81	80	82	2	108	465
81	80	83	2	107.6	507
82	80	83	2	108.53	443
80	83	84	2	116	465
80	83	85	2	122	700
84	83	85	2	120	390
83	85	86	2	124	730
83	85	87	2	115	610
86	85	87	2	120	560
85	87	88	2	108.53	443
85	87	89	2	107	2726.16
85	87	90	2	115	610
88	87	89	2	109	1680.51
88	87	90	2	109	1680.51
89	87	90	2	109	1680.51
87	90	91	2	120	560
87	90	98	2	121	685
91	90	98	2	120	560
90	91	92	2	124	730
90	91	93	2	120	560
92	91	93	2	124	730
91	93	94	2	116	465
91	93	95	2	124	730
94	93	95	2	120	390
93	95	96	2	118	7474.41
93	95	97	2	115	610
96	95	97	2	126	640
95	97	98	2	120	560
95	97	100	2	120	560

98	97	100	2	120	560
90	98	97	2	120	560
90	98	99	2	120	505
97	98	99	2	120	505
97	100	101	2	111.3	632
97	100	102	2	111.3	632
97	100	103	2	111.3	632
101	100	102	2	109	1680.51
101	100	103	2	109	1680.51
102	100	103	2	109	1680.51

[dihedrals]; GROMOS improper dihedrals

ai	aj	ak	al	funct	angle	fc
41	42	40	26	2	0	167.36
40	41	38	31	2	0	167.36
38	40	39	36	2	0	167.36
36	38	37	34	2	0	167.36
34	36	35	32	2	0	167.36
32	34	33	31	2	0	167.36
31	40	32	29	2	0	167.36
29	31	30	27	2	0	167.36
27	29	28	26	2	0	167.36
26	41	27	23	2	0	167.36
21	23	22	19	2	0	167.36
19	21	20	17	2	0	167.36
46	43	47	49	2	0	167.36
47	46	48	55	2	0	167.36
55	47	56	53	2	0	167.36
53	55	54	51	2	0	167.36
51	53	52	49	2	0	167.36
49	46	51	50	2	0	167.36
15	17	16	13	2	0	167.36
13	15	14	11	2	0	167.36
60	57	63	61	2	0	167.36
63	60	64	65	2	0	167.36
65	63	66	67	2	0	167.36
67	65	68	69	2	0	167.36
69	67	70	61	2	0	167.36
61	60	69	62	2	0	167.36
9	11	10	7	2	0	167.36
7	9	8	5	2	0	167.36
3	5	2	4	2	0	167.36
83	80	84	85	2	0	167.36
85	83	86	87	2	0	167.36
90	87	98	91	2	0	167.36
98	90	99	97	2	0	167.36
97	98	100	95	2	0	167.36
95	97	96	93	2	0	167.36
93	95	94	91	2	0	167.36
91	90	93	92	2	0	167.36

[dihedrals]

ai	aj	ak	al	funct	ph0	cp	mult
1	2	3	5	1	180	16.7	2
2	3	5	7	1	0	1	6
3	5	7	9	1	0	3.77	6
7	5	71	74	1	0	5.92	3
5	7	9	11	1	180	33.5	2
10	9	11	13	1	180	1	6
57	11	13	15	1	180	1	6
13	11	57	60	1	0	5.92	3
11	13	15	17	1	180	33.5	2
16	15	17	19	1	180	1	6
43	17	19	21	1	0	3.77	6
19	17	43	46	1	0	5.92	3
17	19	21	23	1	180	33.5	2
22	21	23	26	1	180	1	6
21	23	26	41	1	180	1	6
41	26	27	29	1	180	41.8	2
27	26	41	40	1	180	41.8	2
26	27	29	31	1	180	41.8	2
27	29	31	40	1	180	41.8	2
40	31	32	34	1	180	41.8	2
32	31	40	38	1	180	41.8	2
31	32	34	36	1	180	41.8	2
32	34	36	38	1	180	41.8	2
34	36	38	40	1	180	41.8	2
36	38	40	31	1	180	41.8	2
31	40	41	26	1	180	41.8	2
17	43	46	47	1	180	1	6
49	46	47	55	1	180	41.8	2
47	46	49	51	1	180	41.8	2
46	47	55	53	1	180	41.8	2
46	49	51	53	1	180	41.8	2
49	51	53	55	1	180	41.8	2
51	53	55	47	1	180	41.8	2
11	57	60	63	1	180	1	6
63	60	61	69	1	180	41.8	2
61	60	63	65	1	180	41.8	2
60	61	69	67	1	180	41.8	2
60	63	65	67	1	180	41.8	2
63	65	67	69	1	180	41.8	2
65	67	69	61	1	180	41.8	2
5	71	74	77	1	0	5.92	3
71	74	77	80	1	0	5.92	3

74	77	80	83	1	0	5.92	3
77	80	83	85	1	180	1	6
80	83	85	86	1	180	33.5	2
83	85	87	90	1	180	1	6
85	87	90	98	1	0	3.77	6
98	90	91	93	1	180	41.8	2
91	90	98	97	1	180	41.8	2
90	91	93	95	1	180	41.8	2
91	93	95	97	1	180	41.8	2
93	95	97	98	1	180	41.8	2
95	97	98	90	1	180	41.8	2
98	97	100	101	1	180	1	6

[exclusions]; GROMOS 1-4 exclusions

ai	aj
26	31
26	38
27	32
27	40
29	34
29	38
29	41
31	36
32	38
32	41
34	40
36	41
46	53
47	51
49	55
60	67
61	65
63	69
90	95
91	97
93	98

Table S2. The statistical distribution of each mass-per-length range.

Bin	*Frequency*
0	0
500	1
1000	9
1500	59
2000	468
2500	572
3000	301
3500	351
4000	362
4500	250
5000	114
5500	62
6000	33
6500	20
7000	8
7500	6
8000	14
8500	24
9000	11
9500	11
10000	6
10500	15
11000	59
11500	172
12000	316
12500	352
13000	201
13500	96
14000	65
14500	20
15000	17
15500	4
16000	5
16500	2
17000	0
17500	0
18000	1
More	0

Table S3. The comparsion of structural parameters between NapFF molecule in crystal[2] and simulated NapFF segment in NapFFK_Thy.

Bond

name1	name2	Crystal (nm)	Simulation (nm)
C4	C5	0.1385	0.142
C5	C6	0.1354	0.138
C6	C7	0.1415	0.142
C7	C2	0.141	0.142
C2	C3	0.141	0.142
C3	C4	0.136	0.138
C2	C1	0.1413	0.142
C1	C10	0.1364	0.138
C10	C9	0.1405	0.142
C9	C8	0.1363	0.138
C8	C7	0.1408	0.142
C10	C11	0.1512	0.149
C11	C12	0.1515	0.152
C12	N1	0.1329	0.138
C12	O1	0.1234	0.125
N1	C13	0.1447	0.1435
C13	C14	0.1544	0.153
C14	C15	0.1417	0.149
C15	C16	0.1383	0.139
C16	C17	0.1383	0.139
C17	C18	0.1365	0.139
C18	C19	0.1353	0.139
C19	C20	0.1376	0.139
C20	C15	0.1381	0.14
C13	C21	0.1513	0.156
C21	O2	0.1236	0.125
C21	N2	0.1328	0.138
N2	C22	0.1455	0.1435
C22	C23	0.1541	0.154
C23	C24	0.1511	0.149
C24	C25	0.138	0.139
C25	C26	0.138	0.139
C26	C27	0.1376	0.139
C27	C28	0.1371	0.139
C28	C29	0.1388	0.139
C29	C24	0.1383	0.14
C22	C30	0.152	0.154
C30	O3	0.1211	0.125

Angle

Name1	Name2	Name3	Crystal (°)	Simulation (°)
O3	C30	C22	122.53	121
C30	C22	N2	110.52	111
C30	C22	C23	110.24	109.5
N2	C22	C23	108.32	111
C22	N2	C21	120.32	122
N2	C21	O2	121.14	124
N2	C21	C13	116.05	115
O2	C21	C13	122.7	121
C21	C13	N1	110.86	111
C21	C13	C14	108.65	109.5
N1	C13	C14	110.61	115
C13	N1	C12	122.82	122
N1	C12	O1	122.56	124
N1	C12	C11	115.32	120
O1	C12	C11	122.1	120
C12	C11	C10	111.73	120
C11	C10	C9	120.56	120
C11	C10	C1	120.48	120
C9	C10	C1	118.96	120
C10	C9	C8	120.57	120
C9	C8	C7	121.52	120
C8	C7	C6	123.4	120
C8	C7	C2	118.25	120
C6	C7	C2	118.4	120
C7	C6	C5	121.4	120
C6	C5	C4	119.8	120
C5	C4	C3	121.2	120
C4	C3	C2	120.4	120
C7	C2	C3	118.82	120
C7	C2	C1	118.88	120
C3	C2	C1	122.27	120
C10	C1	C2	121.8	120
C13	C14	C15	111.81	111
C14	C15	C16	120.48	120
C14	C15	C20	122.3	120
C16	C15	C20	117.13	120
C15	C16	C17	121.99	120
C15	C20	C19	120.3	120
C20	C19	C18	121.1	120
C19	C18	C17	119.2	120
C16	C17	C18	120.1	120
C22	C23	C24	112.68	111

C23	C24	C29	120.88	120
C23	C24	C25	120.47	120
C29	C24	C25	118.64	120
C24	C29	C28	120.97	120
C24	C25	C26	120.71	120
C25	C26	C27	119.6	120
C26	C27	C28	120.44	120
C29	C28	C27	119.65	120

Dihedral

Name1	Name2	Name3	Name4	Crystal (°)	Simulation（°）
O3	C30	C22	N2	136.141	180
C23	C22	N2	C21	170.535	180
N2	C22	C23	C24	168.782	0
C22	N2	C21	C13	166.875	180
O2	C21	C13	N1	34.965	180
C14	C13	N1	C12	134.481	0
N1	C13	C14	C15	-62.421	0
C13	N1	C12	C11	-174.896	180
O1	C12	C11	C10	-99.616	180
C12	C11	C10	C1	71.703	180
C1	C10	C9	C8	1.374	180
C9	C10	C1	C2	-0.279	180
C10	C9	C8	C7	-1.039	180
C9	C8	C7	C2	-0.391	180
C2	C7	C6	C5	-0.229	180
C6	C7	C2	C3	0.259	180
C7	C6	C5	C4	-0.046	180
C6	C5	C4	C3	0.296	180
C5	C4	C3	C2	-0.26	180
C4	C3	C2	C7	-0.022	180
C7	C2	C1	C10	-1.132	180
C13	C14	C15	C16	96.28	180
C20	C15	C16	C17	0.354	180
C16	C15	C20	C19	2.051	180
C15	C16	C17	C18	-1.861	180
C15	C20	C19	C18	-3.009	180
C20	C19	C18	C17	1.443	180
C19	C18	C17	C16	0.943	180
C22	C23	C24	C25	71.117	180
C25	C24	C29	C28	-0.426	180
C29	C24	C25	C26	0.001	180
C24	C29	C28	C27	0.395	180
C24	C25	C26	C27	0.453	180
C25	C26	C27	C28	-0.487	180
C26	C27	C28	C29	0.068	180
C2	C1	C3	C7	1.277	0
C7	C2	C6	C8	0.525	0
C10	C1	C9	C11	0.281	0
C12	C11	O1	N1	0.768	0
C15	C14	C16	C20	-1.924	0
C21	C13	O2	N2	2.399	0
C24	C23	C25	C29	-1.924	0

Reference

(1) Y. Gao, R. Nieuwendaal, E. K. Dimitriadis, B. Hammouda, J. F. Douglas, B. Xu and F. Horkay, *Gels,* 2016, **2**, 27.

(2) Z. M. Yang, G. L. Liang, L. Wang and B. Xu, *J. Am. Chem. Soc.,* 2006, **128**, 3038-3043.